PARAMETRIC ANALYSIS OF AN L-BAND DEPLOYABLE OFFSET REFLECTOR FOR CUBESATS

Mario Mendez-Soto, Adrián Márquez-Alperi, Elena Fernández-Niño, Adriano Camps, *Fellow, IEEE*

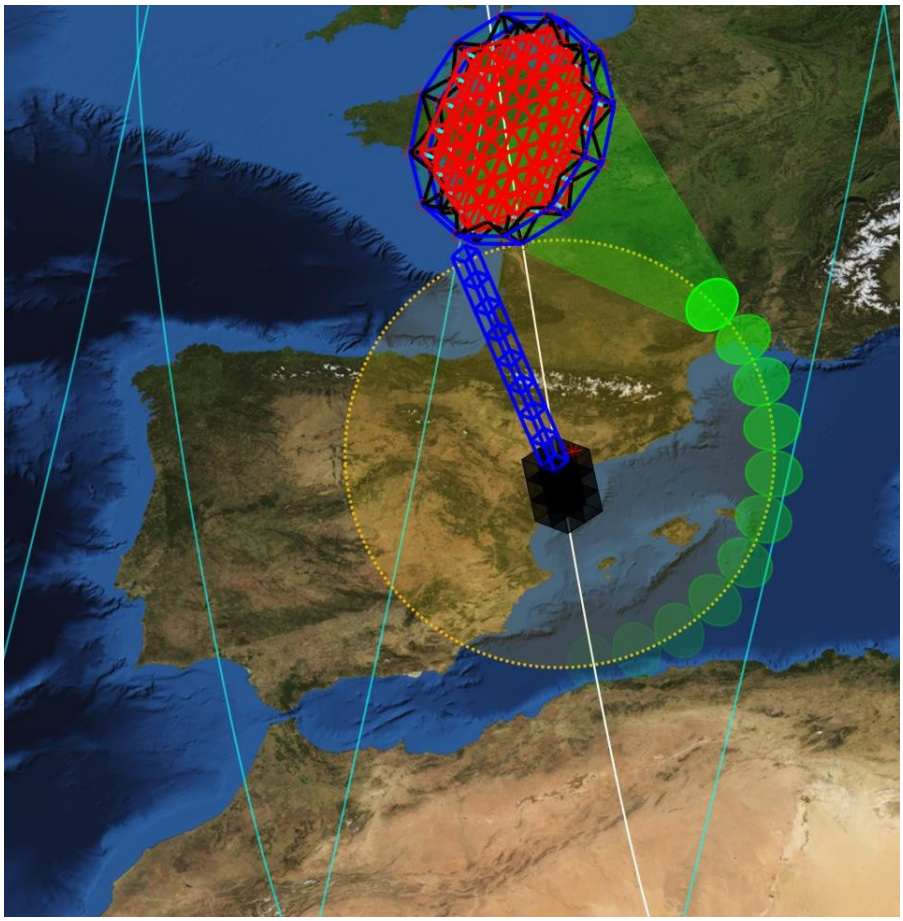

Artist view of the deployable reflector antenna in a 12U CubeSat.

Take-Home Messages

- Earth observation microwave radiometer payload based on an L-band deployable offset reflector for CubeSat.
- Optimal offset reflector configuration analyzed has a circular shape and regular mesh.
- Regular meshes perform better than irregular ones, but the required supporting structure is larger.

 DOI 10.1109/JMASS.2020.3002339

PARAMETRIC ANALYSIS OF AN L-BAND DEPLOYABLE OFFSET REFLECTOR FOR CUBESATS

Mario Mendez-Soto, Adrián Márquez-Alperi, Elena Fernández-Niño, Adriano Camps, *Fellow, IEEE*

Abstract Thanks to the advances in the miniaturization and improved power consumption efficiency of electronics, computers, cell phone technologies… today's spacecrafts and payloads are reducing their size and increasing their performance. However, not all systems can be reduced, as their dimensions are determined by the laws of Physics. This study is focused the design of an L-band reflector antenna for a CubeSat-based Earth Observation mission devoted to measure the surface soil moisture. Two configurations of deployable parabolic reflector antennas and meshes are presented from the mechanical point of view. The electromagnetic analyses including the antenna feeder are also presented. It is found that the regular circular mesh performs slightly better than the irregular one, although requires a more careful manufacturing process.

Keywords **— CubeSat, deployable reflector, errors, electromagnetic analysis, mechanical design, mesh.**

I. INTRODUCTION

THE CubeSat standard was introduced in 1999 by Profs. Bob Twiggs and Jordi Puig-Suari from Stanford University and the California Polytechnic State University, respectively. The CubeSat satellite consists of a cube (1U) of 10 cm side with a maximum weight of 1.33 kg [1]. At the present time, the largest standardized CubeSat is the 3x2U, or 6U [1]. Even so, 8U, 12U and 16U have also been commercialized, i.e. [2].

The CubeSat standard was firstly oriented for academic purposes to give students the opportunity to have their first contact with space technology by working in real space missions. Later, the standard began also to be commercialized and used in commercial projects. Currently, the most widely used structure is the 3U CubeSat, because only two companies have put in orbit a very large number of 3U CubeSat constellations: 387 by Planet Labs equipped with optical sensors, and 115 by Spire Global using GNSS-Radio Occultation receivers, both for Earth Observation [3].

Nowadays, technology incorporated in satellites is increasingly thanks to the miniaturization of electronic components and the improvement of their efficiency, especially in terms of power consumption. Therefore, achieving a good system performance and obtaining a great advantage in terms of satellite space optimization. So far, since the spacecraft size is ultimately determined by the mission requirements, many Earth Observation and communication missions cannot be fulfilled because of the limited availability of deployable reflectors for CubeSats (i.e. the largest one, to the authors' knowledge, is just 0.5 m in diameter [4,5]).

However, new engineering approaches have been studied to overcome the borderline between the current technological limits and the new and ambitious space goals.This new area under development is antenna reflector systems for CubeSat applications. In general, thedevelopment of satellite reflector antennas began back to 1974 [5], with several missions that incorporated large deployable reflectors for different applications. To this day, the American satellite TerreStar-1, an 18 m diameter reflector developed to provide communications services, is the largest deployable reflector ever launched [6].

Multiple approaches have been proposed for the structure and deployment of satellite reflector antennas [5]:

- Umbrella-like structure using a directly connected metallic mesh.
- Umbrella-like structure supporting a tensioned-cable network that shapes the reflecting surface.
- Tensioned-cable network shaping the reflecting surface and supported by a deployable truss structure.
- Tensioned-cable network shaping the reflecting surface and supported by a deployable hoop structure.
- Flower pod structure.
- Umbrella-like structure using highly flexible and compliant radial ribs.
- Deployable tensegrity structure.

Although several of these methods have been successfully implemented for large deployable reflectors, such as the SMAP's reflector (a 6-m of diameter reflector with a weight of 944 kg [7]), not all of them are suitable for CubeSat

This work received funding from "CommSensLab" Excellence Research Unit Maria de Maeztu (MINECO grant MDM-2016-0600), and the 2014 ICREA Academia award to Prof. Camps by the Generalitat de Catalunya.

Mario Mendez-Soto is a graduate student at the Institut für Mechanik (Bauwesen) of Universität Stuttgart, Stuttgart 70569 Germany (e-mail: st170421@stud.uni-stuttgart.de) and the International Centre for Numerical Methods in Engineering (CIMNE) at Universitat Politècnica de Catalunya—BarcelonaTech (UPC), 08034 Barcelona, Spain (mario.alberto.mendez@upc.edu).

Adrián Marquez-Alperi and Elena Fernández-Niño are members of the CommSensLab – UPC, "María de Maeztu" Excellence Research Unit, Dept. of Signal Theory and Communications, Universitat Politècnica de Catalunya—BarcelonaTech (UPC), 08034 Barcelona, Spain (e-mail: adrian.marquez.alperi@estudiant.upc.edu; elena.fernandez.nino@estudiant.upc.edu)

Adriano Camps is the scientific coordinator of the CommSensLab – UPC, "María de Maeztu" Excellence Research Unit, Dept. of Signal Theory and Communications, Universitat Politècnica de Catalunya— BarcelonaTech (UPC), 08034 Barcelona, Spain (e-mail: camps@tsc.upc.edu).

missions. The 50 cm diameter RainCube's reflector [4], is – to the authors' knowledge – the only deployable parabolic antenna for CubeSats with flight heritage.

There are several companies all over the world currently on the race to develop and commercialize CubeSat deployable reflector antennas. For instance, the US-based company TENDEG [8] has developed two deployable antenna reflectors of 0.5 m and 1-to-3 m of diameter, focused both on CubeSat missions. Likewise, the Asian company NSLComm also offers antenna reflectors for small satellites [9]. Conversely, up to date there are no European CubeSat reflector antennas which are commercially available.

Following the current trend, UPC NanoSat Lab [10] is currently designing an Earth Observation mission to measure surface soil moisture using an L-band (1.4 GHz) microwave radiometer with conical scan and applying a pixel downscaling technique [11]. In this study a 1-m deployable reflector is presented including the design trade-offs and the electromagnetic analysis. The possibility of adapting such technology for small satellites is the novelty of the current work which aims to provide a first approximation to the feasibility of the design and exploitation of a European deployable reflector antennas for CubeSat applications.

II. Geometry and Configuration of Antenna Reflectors

Antenna reflectors are geometrically described considering two parent surfaces: a paraboloid with focus *f,* and a cylindrical surface with diameter *D* with an axis usually parallel to the axis of the paraboloid. Hence, the reflector contour is defined by the intersection of these two parent surfaces [12]. Moreover, the geometry of the reflectors can be modified by changing the relative position of the parent surfaces. Thus, the geometry is fully characterized by the parameters of the parent surfaces and, additionally, by the offset distance *E* (or alternately an offset angle φ), and the angle between the axes of the parent parabolic and cylindrical surfaces (see Fig. 1).

If the offset distance and the angle between the axes of the parent surfaces are both equal to zero, the reflector antenna is axisymmetric, and its contour is circular both in global and local coordinate systems. Despite its simple geometry, it results in a structure which is frequently bulky, and the antenna feeder blocks the aperture which leads to poorer electromagnetic performance [12], especially at low frequency bands. Given this undesired effect at low frequencies, parabolic reflectors are usually designed with a non-zero offset distance [13].

Offset reflectors with *standard* configuration [12] are characterized by parent surfaces whose axes have the same direction (*z*-direction in the case of Fig. 1a).

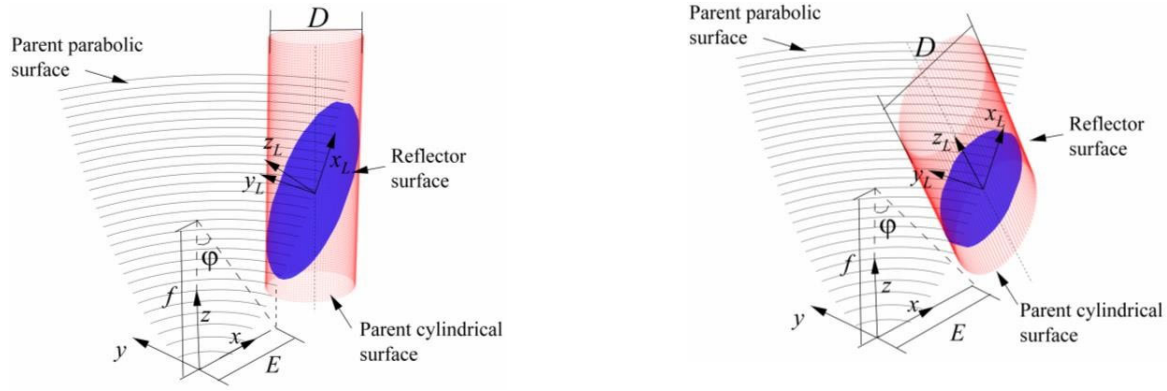

(a) Standard configuration (b) Circular configuration

Fig. 1. Geometry of offset reflectors and configurations

This type of configuration generates a contour with coplanar points in an elliptical curve. From a practical engineering point of view, elliptical rims come with important difficulties especially during the structural design and the deployment analysis. An alternative configuration with a projected circular contour was suggested in [14]. The result is a much simpler structure with a better pre-stress distribution and hence efficient structural design. Fig. 1b depicts how this configuration is achieved when the local axis of the reflector z_L coincides with the axis of the cylindrical surface.

III. Design Approach and Constraints

A. Geometric and structural design

As described in Section II, parameters *f* and *D* (or alternatively within the framework of this article a focal ratio *r* defined as *f*/*D*), and the offset angle φ fully characterize the geometry of an offset reflector.

Nevertheless, it is important to consider in the design that the CubeSat mission will include a 1-to-3-meter deployable scanning reflector, and a feedhorn which will spin relative to the spacecraft. Such a structure entails the need of taking measures to compensate the exerted torque and to reduce wobbling once equilibrium is reached. As shown in [13], a stable rotating structure is obtained if the components are

distributed in such a way that the net torque around the center of mass is minimum [15].

Predicting the mass distribution for preliminary prototypes is a challenging task, however design considerations towards a uniform distribution can be taken. Neglecting the mass of the deployable mast, the center of mass of the system is very close to the geometric center of the reflector and, therefore, arranging a uniform mass distribution is achievable by establishing a relationship between the geometric parameters r and φ. This relationshipguarantees a minimum distance x_s between the geometric center of the reflector and the axis of rotation (which usually goes through the focal point and it is perpendicular to the reflector). Consequently, having selected a focal ratio r, an optimized offset angle φ can be computed (see Fig 2.).

A second group of design parameters includes those that define the structural configuration of the reflector's supporting truss. Overall, these parameters will determine the mechanical and structural complexity of the system and will have an important effect on the surface accuracy of the reflecting surface and, therefore, on the electromagnetic performance of the antenna.

The main structural parameters are depicted in Fig. 3. The following are considered structural design parameters:

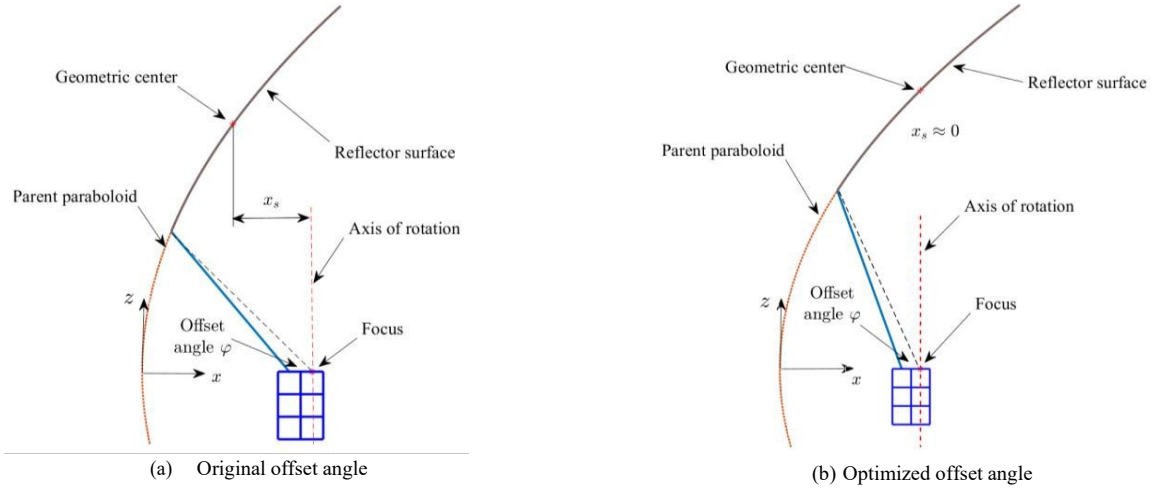

(a) Original offset angle (b) Optimized offset angle

Fig. 2. CubeSat planar configuration and offset prediction

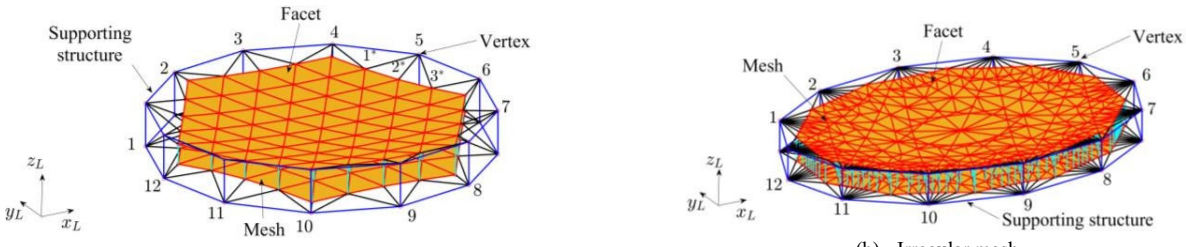

(a) Regular mesh (b) Irregular mesh

Fig. 3. Main structural parameters of the reflector

1. Mesh type (refer to Section B for a detailed description): regular (Fig. 3a) and irregular (Fig. 3b).

2. Number of ring vertices or truss elements, n (irregular mesh). The structures shown in Fig. 3 have 12 vertices.

3. Number of soft divisions per side, n_s (regular mesh). The regular mesh in Fig. 3a has 3 soft divisions per side.

B. Mesh design and surface accuracy

In real engineering applications, reflectors deviate from the ideal parabolic surface. This is because the surface is not continuous, but it is approximated using a mesh of polygonal facets. The deviation between the mesh facets and best-fit parabolic surface is called *systematic faceting error*, and it is a specified design requirement since a high deviation deteriorates the overall electromagnetic performance. Other deviation sources such as manufacturing, loading and random surface errors are not considered in the present study.

The so-called best-fit parabola can be expressed as:

$$z_{bf} = \sqrt{\left(x^2 + y^2\right) / \left(4\left(f + \Delta f\right)\right)} + \Delta z, \qquad (1)$$

where Δf and Δz denote the variation in the focal length and a translation in the z-direction of the original standard surface, respectively. Values for Δf and Δz are determined by standard optimization algorithms from the fit of the geometric centers of the polygonal facets (see Fig. 4).

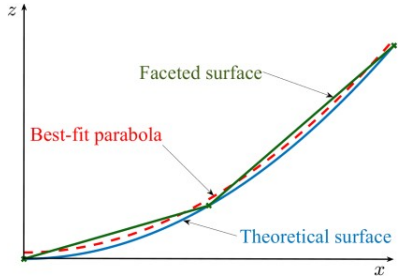

Fig. 4. Best-fit parabolic surface

Once the faceted mesh has been constructed, the deviation is characterized using the root mean square (RMS) error between the surfaces (δ_{rms}). This error is computed in the global coordinate system using the following expression:

$$\delta_{rms} = \sqrt{\frac{\sum_{i=1}^{n_f} A_i (z_i - z_{bf_i})^2}{\sum_{i=1}^{n_f} A_i}}, \qquad (2)$$

where n_f is the number of facets, z_i is the z-coordinate of a point located on the planar interpolation of the facet, z_{bfi} is the corresponding z-coordinate in the best-fit paraboloid and A_i is the projection onto the XY plane of the facet area.

During the design of any reflector surface two main tasks are required to be addressed. Firstly, a mesh must be constructed for a fully deployed configuration for a given desired surface and with a given maximum allowable systematic error. Secondly, engineers must select materials and a structural configuration such that, when fully deployed and under the operational rotational loadings, the deformed surface only deviates from the ideal surface within a range of allowable tolerance [16]. Within the framework of the current study, only the first task is considered.

For the construction of the faceted mesh two different approaches are considered:

1 – A **regular mesh** with a geodesic pattern and constructed using the six-ring tension method as described in [14]. This type of mesh has nearly equilateral triangular facets as shown in Fig. 3a and by increasing the number of soft divisions n_s the systematic error can be reduced. However, the use of soft connections between the cables adds complexity to the manufacturing process. One of the main advantages of the regular mesh is the presence of boundary cables (black colored area in Fig. 3a) which allowthe contour points to be non-coplanar. Thus, regular meshescan be used for both standard and circular configurations.

2 – An **irregular mesh** constructed using the method originally proposed in [17] for axisymmetric reflectors. The construction process is schematically shown in Fig. 5 for vertices 1 and 4. As depicted in Fig. 5, the mesh is defined by the connections from each vertex to every other vertex (with the exception of the adjacent vertices) in the polygon. The intersections (blue dots in Fig. 5) correspond to the mesh positions that are assumed to match the theoretical parabolic surface. Given the absence of boundary cables, this configuration requires coplanarity of all the vertices, therefore it is only suitable for standard configuration. Moreover, it must be noted that for the deviation estimation only the reflector's central area will be considered (red colored in Fig. 3b), and the area adjacent to the supporting structure (black colored in Fig. 3b) is neglected. This will require adjusting the input diameter to match a specific desired diameter or area.

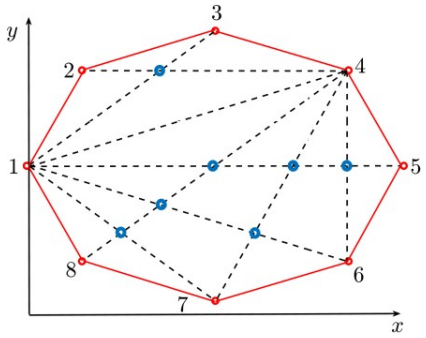

Fig. 5. Construction process for irregular mesh

To study the effect of the design parameters on the surface accuracy, the following sample reflector is considered: 1-m^2 offset reflector with focal length of 0.75 m, two different configurations (circular with regular mesh and standard with irregular mesh), 12 truss elements (n ring vertices), and 6 soft divisions for the regular mesh (n_s). Numerical results are summarized in Table I.

TABLE I
NUMERICAL RESULTS FOR 1-M^2 REFLECTOR

Parameter	Case 1	Case 2
Mesh	Regular	Irregular
Configuration	Circular	Standard
Height of supporting structure [cm]	19.1	14.8
Number of mesh nodal points	169	301
Diameter [m]	1.23	1.09
Maximum error [mm]	0.54	1.24
Root mean square error [mm]	0.29	0.36

Furthermore, the surface error patterns for both cases are shown in Fig. 6. Please note that only the central area of the mesh is depicted (red colored in Fig. 3), whereas the area adjacent to the supporting structure (black colored in Fig. 3) is ignored.

Table I shows that the irregular mesh entails a higher maximum and RMS error is compared to the regular mesh. However, the distribution of the error in Fig. 6b illustrates that the most critical areas, where the nodes (intersections) density is lower, are at the center whereas the peripheral parts have significantly lower deviation. Conversely, for the regular mesh (see Fig. 6a) the deviation distribution is nearly uniform with higher error on the left which is due to the larger curvature of the parent paraboloid in this region. As the results show the supporting structure would fit into a 2U and 1.5U for the regular and irregular mesh, respectively. Moreover, the number of nodal points needed for the irregular mesh (301) is approximately twice the number of nodes required in the regular mesh (169).

For a better understanding of the overall effect of the multiple design parameters, parametric sweeps can be performed to find optimal combination that leads to high-accuracy surfaces while not compromising the structural complexity of the reflector. Fig. 7 illustrates the evolution of the RMS error for different f/D ratios varying the number of vertices (n) for irregular meshes, and the number of soft divisions (n_s) for regular meshes. As in the previous results,

the irregular meshes were constructed for a standard configuration whereas a circular configuration was selected for the regular meshes.

Data suggests that the error reduces as the focal ratio becomes larger (i.e. the supporting structure is flatter) and, as expected, it also diminishes with increasing n and n_s. Nevertheless, it is important to note that for regular meshes there is a proportionality between the number of vertices and the number of soft divisions needed which ultimately depends on the design of the boundary cables between the mesh and its supporting structure. The larger the number of vertices, the less compact the supporting structure becomes thus impacting the volume required in the spacecraft.

Considering this, a suitable connection pattern between the mesh and the supporting structure must be designed to properly match the selected mesh while not compromising the overall reflector compactness.

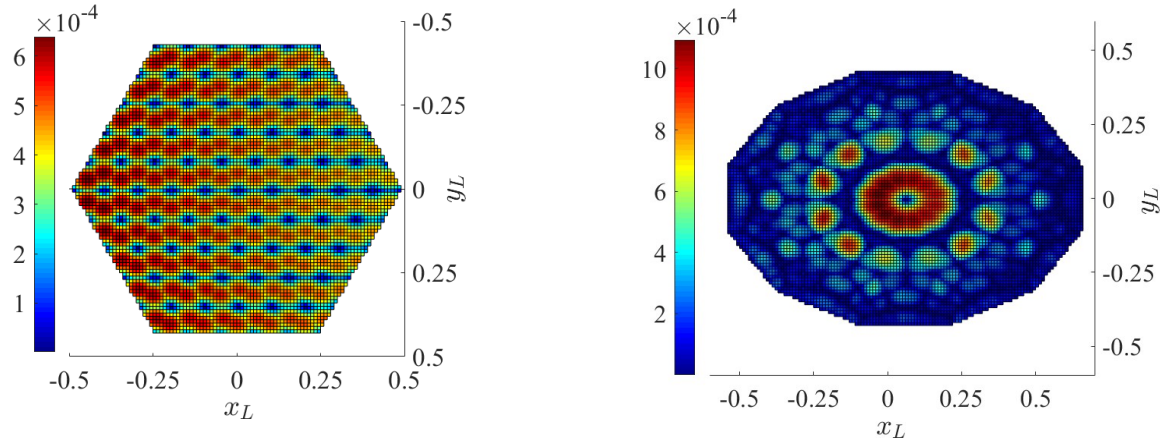

(a) Regular Mesh (b) Irregular mesh

Fig. 6 - Error distribution in [m] for 1-m^2 reflector antenna with two different meshes

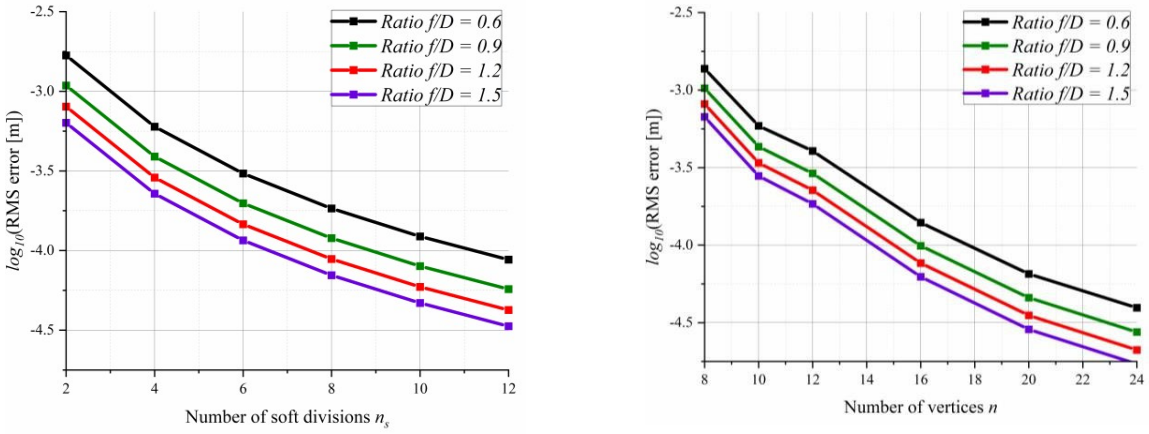

(a) Regular mesh with circular configuration (b) Irregular mesh with standard configuration

Fig. 7 - RMS error pattern for two different mesh types

IV. Antenna Feed

A. Feed Design

For the sake of simplicity, weight, volume and reduced back radiation, the selected reflector feed is a dual-polarization microstrip patch antenna. In order to achieve the dual-polarization, the antenna is fed with two (Fig 8.a - c) or four (Fig 8.b - d) probes.

Assuming a Rogers RT5880 ($\varepsilon_r = 2.2$, $\tan_d = 0.0009$), with a thickness of 3.175 mm, the patch dimensions for the case of two probes are 67.88 mm x 67.88 mm while 68.30 mm x 68.30 mm are the ones for the four-probe case. Probes are 11.2 mm and 10.8 mm away from the center, respectively for a 50 Ω matching. The size of the ground plane has been limited to 94 mm x 94 mm, which is the internal size of the CubeSat PCBs (PC/104 PCB form factor).

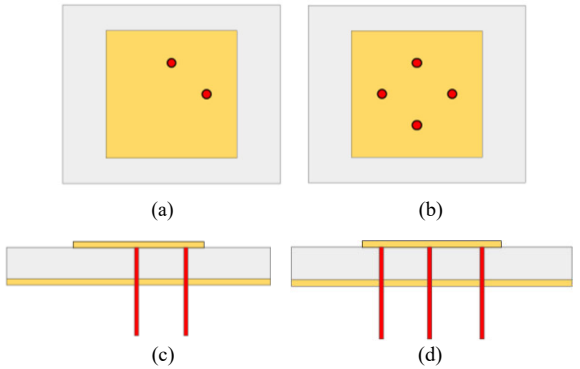

Fig. 8 -. Feed antenna views. (a) Top view with 2 probes. (b) Top view with 4 probes. (c) Side view with 2 probes. (d) Side view with 4 probes.

B. Electromagnetic Behavior

The electromagnetic analysis has been conducted using CST Studio Suite [18].

Fig. 9 shows the simulation results for both patches (2 and 4 probes). The patch is tuned at 1413 MHz and the return losses (S_{11}) are smaller than 10 dB over a bandwidth of 26.1 and 22.2 MHz for the case of 2 and 4 probes respectively, while the isolation between ports (S_{21}) is better than -35 dB over the whole bandwidths.

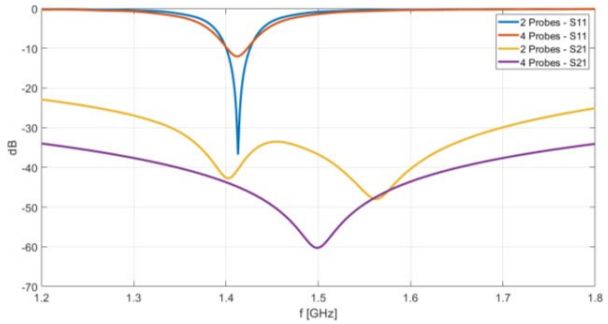

Fig. 9 - Return losses (S_{11}) and isolation (S_{21}) of the 2- and 4-probe antenna.

Fig. 10 shows a comparison of the co- and cross-polarization when using both, 2 and 4 probes. The goal of using 4 probes is to reduce the cross-polarization level. Table II summarizes the main results for both configurations.

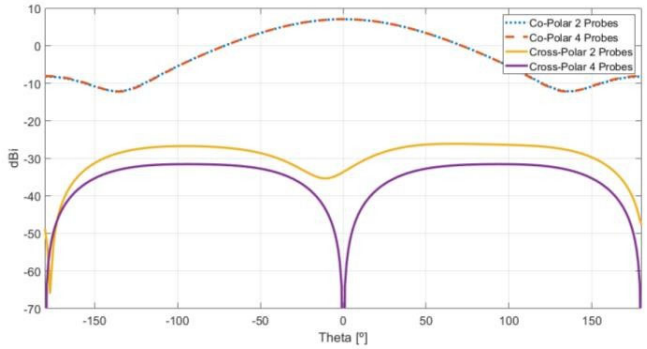

Fig. 10 - Co- and cross-polarization comparison (ϕ=90º) of the 2- and 4-probe antenna.

TABLE II
PATCH ANTENNA PROBES METHOD COMPARISON

Parameter	*2 probes*	*4 probes*
Directivity [*dBi*]	7.06	7.08
Radiation Efficiency [%]	95.0	88.8

While the analysis shows that the insertion losses are smaller for the 2 probes patch antenna, the cross-polarization is significantly smaller for the 4 probes patch. Nevertheless, the selection between the 2 and 4 probes is conducted in Section V, taking into account the reflector itself.

V. Electromagnetic Analysis

The performance of both reflectors is analyzed: standard configuration with irregular mesh, and circular configuration with regular mesh.

The analysis is conducted assuming that the reflector and feeder are in the top of the 4U side of a metallic 12U CubeSat structure. To make a fair comparison, both reflectors have the same surfaces (1 m^2).

It is important to note that the electromagnetic simulation is not assuming a smooth surface, but the mesh with triangular facets including the sides, and the diffraction produced by these discontinuities.

Figures 11a and 11b show the comparison of the co- and cross-polarization patterns. Figures 12a-d show the radiation pattern in uv coordinates, for the 2- or 4-probe patches, for both the standard configuration with irregular mesh, and the circular configuration with regular mesh, respectively. Since offset reflectors induce a larger cross-polarization than axis-parabolic ones, the differences between the 2- and 4- probes are negligible. Tables III and IV summarize the main results for both configurations.

TABLE III
L-BAND SIMULATED FARFIELD PARAMETERS FOR 1-M² STANDARD CONFIGURATION (301 NODAL POINTS) WITH THE 12U STRUCTURE

Parameter	*2 Probes*	*4 Probes*
Directivity [*dBi*]	18.48	18.47
Side Lobe Level [*dB*]	14.58	13.45
F/B Ratio[*dB*]	16.36	15.42
Radiation Efficiency [%]	94.91	83.17
Main Beam Efficiency [%]	67.58	68.34

TABLE IV
L-BAND SIMULATED FARFIELD PARAMETERS FOR 1-M² CIRCULAR CONFIGURATION (169 NODAL POINTS) WITH THE 12U STRUCTURE

Parameter	*2 Probes*	*4 Probes*
Directivity [*dBi*]	18.60	18.61
Side Lobe Level [*dB*]	13.83	14.11
F/B Ratio[*dB*]	15.9	15.55
Radiation Efficiency [%]	94.98	83.23
Main Beam Efficiency [%]	67.94	66.54

As it can be appreciated, both reflectors perform in a very similar way. The circular configuration with regular mesh shows a slightly better directivity and radiation efficiency, while the best main beam efficiency level is for a 4-probe patch with standard configuration and irregular mesh.

VI. Conclusions

Since the first CubeSat standard, CubeSats have passed from the academic to the commercial world. The technology boarded in these small satellites has benefited from the miniaturization and improved power consumption efficiency of electronics, computers, cell phone technologies… but some structures cannot be reduced in size. It is interesting to study large deployable reflectors that can offer new and ambitious challenges in future space missions, either for Earth observations, or communication missions.

The first efforts towards the design of a rotating offset parabolic reflector for CubeSat applications are presented, including the trade-off between two different faceted meshes, and the assessment of the RMSE wrt the best-fit parabolic surface. The study shows that a circular

configuration with regular mesh can provide better results in terms of surface accuracy. Nevertheless, a regular mesh requires a supporting structure which is larger in comparison with the supporting structure of the irregular mesh. Additionally, results of the parametric analysis illustrate the variation of the systematic error when the main design parameters are changed.

The electromagnetic analysis of a $1m^2$ deployable reflector at L-Band shows satisfactory results and demonstrates a similar performance for both cases. Although the performance of such a reflector antenna will start degrading at high frequency bands (e.g. C band), future analysis must be conducted in order to select the most efficient reflector antenna in terms of manufacturing and deployment capacity.

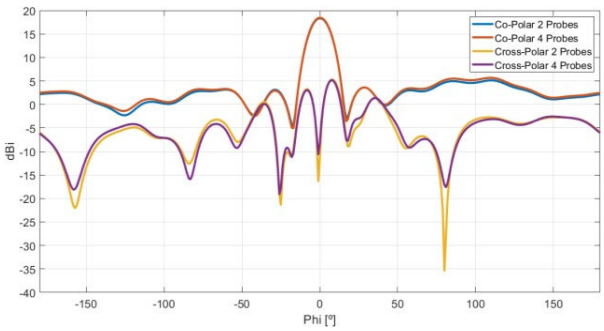

Fig. 11a - 2-probes vs 4-probes - Co-Polar vs Cross-Polar for Standard configuration and irregular mesh (θ=90º).

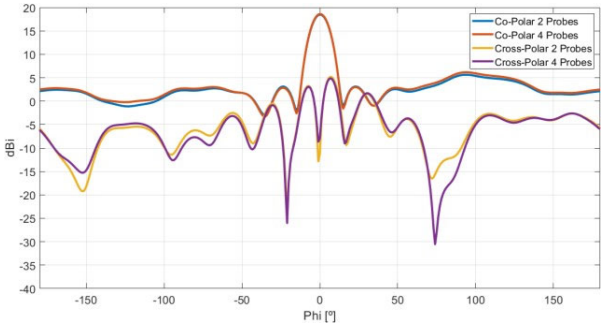

Fig. 11b - 2-probes vs 4-probes - Co-Polar vs Cross-Polar for Circular configuration and regular mesh (θ=90º).

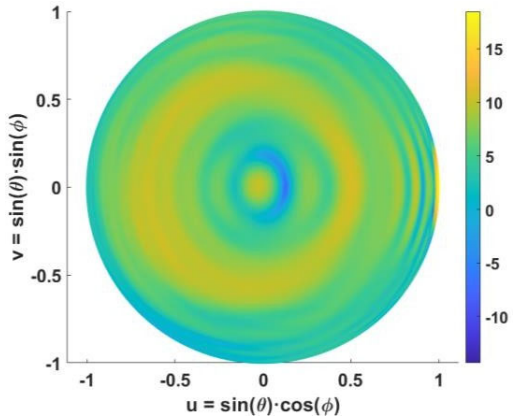

Fig. 12a - 2-probes radiation pattern for Standard configuration and irregular.

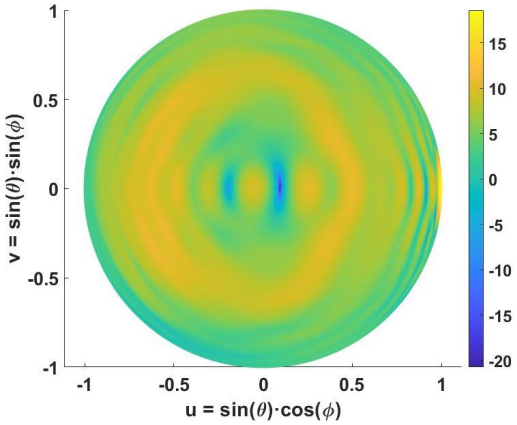

Fig. 12b - 2-probes radiation pattern for Circular configuration and regular.

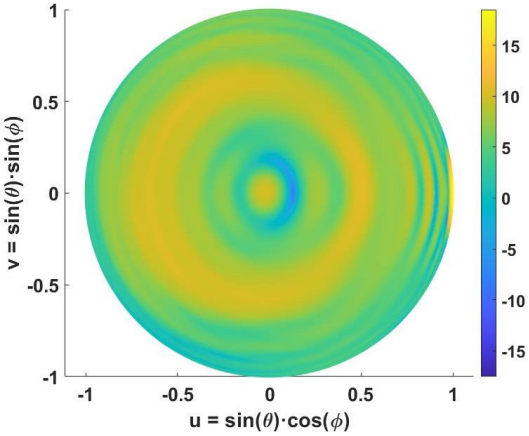

Fig. 12 -. 4-probes radiation pattern for Standard configuration and irregular.

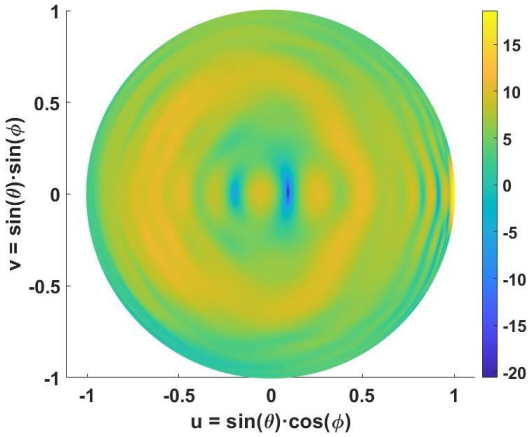

Fig. 12 -. 4-probes radiation pattern for Circular configuration and regular.

REFERENCES

[1] CubeSat Design Specification (Revision 13 - Updated 6 April 2015). Available at: http://www.cubesat.org/resources, last visited March 2nd, 2020.

[2] ISIS CubeSat Structures. Available at: https://www.isispace.nl/products/cubesat-structures/, last visited March 2nd, 2020.

[3] Nanosats Database. Available at: https://www.nanosats.eu/cubesat, last visited March 2nd, 2020.

[4] Jet Propulsion Laboratory - California Institute of Technology, Radar in a CubeSat (RainCube), October 2019. Available at: https://www.jpl.nasa.gov/cubesat/missions/raincube.php, last visited March 2nd, 2020.

[5] J. Nieto, D. Valcázar, A. Martínez, A. Camps, F. Deconinck, "Large Deployable Offset Fed Antennas for CubeSats", *40th ESA Antenna Workshop*, 8-10 October 2019, ESTEC, Noordwijk, the Netherlands (in press).

[6] NASA Space Data Coordinated Archive. TerreStar 1. Available at: https://nssdc.gsfc.nasa.gov/nmc/spacecraft/display.action?id=2009-035A, last visited May 21st, 2020.

[7] Jet Propulsion Laboratory - California Institute of Technology, Specifications SMAP-Soil Moisture Active Passive, August 2019. Available at: https://smap.jpl.nasa.gov/observatory/specifications/, last visited March 2nd, 2020.

[8] TENDEG – Space Antennas and Deployables. Available at: https://www.tendeg.com/products, last visited on May 21st, 2020.

[9] NSLComm - Nano Satellites High Bandwidth Communication Systems. Available at: https://www.nslcomm.com/product, last visited on May 21st, 2020.

[10] UPC NanoSatLab web page. Available at: https://nanosatlab.upc.edu/en, last visited March 2nd, 2020.

[11] E. Santi, M. Brogioni, G. Macelloni, S. Paloscia, P. Pampaloni and S. Pettinato, "A simple technique to improve the AMSR-E spatial resolution at C-band," *2008 Microwave Radiometry and Remote Sensing of the Environment*, Firenze, 2008, pp. 1-4.

[12] T. Milligan, *Modern Antenna Design*. 2nd ed., ed. John Wiley & Sons, Inc., New Jersey, pp. 380-390, 1982.

[13] G. Tilbert, "Deployable Tensegrity Structure for Space Applications", Ph.D. Thesis, Royal Institute of Technology, Stockholm, Sweden, 2002. Available online at: http://www-civ.eng.cam.ac.uk/dsl/publications/TibertDocThesis.pdf, last visited March 2nd, 2020.

[14] C.Y. Lai, S. Pellegrino, "Shape and stress analysis of offset CRTS reflectors". Cambridge, UK: Department of Engineering, University of Cambridge; 1999. Report No. CUED/D-STRUCT/TR177.

[15] M. Mobrem, S. Kuehn, C. Spier, E. Slimko, "Design and Performanceof Astromesh Reflector Onboard Soil Moisture Active Passive Spacecraft", *IEEE Aerospace Conference 2012*, Big Sky, MT, 2012, pp. 1-10.

[16] H. Shi, Y. Sichen, Y. Bingen, "New Methodology of Surface Mesh Geometry Design for Deployable Mesh Reflectors", *Journal of Spacecraft and Rockets*, Vol. 55, No. 2, pp. 266-282, March–April 2018.

[17] S. Bolton, D. Doty, P. Rivera, "Compact Deployable Antenna for CubeSat Units." Project Report. NASA Jet Propulsion Laboratory and California Polytechnic State University; California, 2014-2015.

[18] CST STUDIO SUITE. Available at: https://www.3ds.com/products-services/simulia/products/cst-studio-suite/, last visited March 25th, 2020

Mario Mendez-Soto is a second-year student of the International Master's Programme in Computational Mechanics of Universitat Politècnica de Catalunya - BarcelonaTech and Universität Stuttgart. He will graduate in 2020. He received a bachelor's degree in Aircraft Engineering from Samara National Research University in the Russian Federation in 2017. He is member of the Central American Association for Aeronautics and Space (ACAE).

Adrián Márquez-Alperi was born in Asturias, Spain in October 18, 1996. He received a bachelor's degree in Telecommunication Technologies and Services Engineering at the Polytechnic School of Engineering of Gijón in the branch of Signal Theory and Communications in 2018. Currently, he is a second-year student of the master's degree in Telecommunications Engineering with specialization in Antennas, Microwaves and Photonics for Earth Observation at the Polytechnic University of Catalunya. He will graduate in February 2021. He is currently working on deployable antennas for CubeSats at NanoSat Lab in Barcelona.

Elena Fernández-Niño received the B.S. degree in Telecommunications Technologies and Services Engineering, specialized in the field of telecommunications systems, from Polytechnic University of Catalonia, Barcelona, Catalonia, Spain, in 2019. Since 2019 she is a first-year student of the master's degree in Telecommunications Engineering, specialized in antennas, microwaves and photonics for communications and Earth observation, at Polytechnic University of Catalonia, Barcelona, Catalonia, Spain. She will graduate in 2021. During her bachelor's Thesis conducted a feasibility Earth observation mission analysis using passive microwave radiometry from a CubeSat, NanoSat Lab-UPC, Barcelona Spain. Since then, she is member of NanoSat Lab-UPC working as an assistant professor designing and testing CubeSat missions, Barcelona Spain.

Prof. Adriano Camps was born in Barcelona, Spain, in 1969. He received the degree in Telecommunications Engineering and a Ph.D. degree in Telecommunications Engineering from the Universitat Politècnica de Catalunya (UPC), Barcelona, Spain, in 1992 and 1996, respectively. In 1991 to 1992, he was at the ENS des Télécommunications de Bretagne, France, with an Erasmus Fellowship. Since 1993, he has been with the Electromagnetics and Photonics Engineering Group, Department of Signal Theory and Communications, UPC, where he was first Assistant Professor, Associate Professor in 1997, and Full Professor since 2007. In 1999, he was on sabbatical leave at the Microwave Remote Sensing Laboratory, of the University of Massachusetts, Amherst. Since 1993, he has been deeply involved in the European Space Agency SMOS Earth Explorer Mission, from the instrument and algorithmic points of view, performing field experiments, and since 2001 studying the use of GNSS-R techniques to perform the sea state correction needed to retrieve salinity from L-band radiometric observations. His research interests are focused in microwave remote sensing, with special emphasis in microwave radiometry by aperture synthesis techniques and remote sensing using signals of opportunity (GNSS-R). He has published over 203 papers in peer-reviewed journals, 6 book chapters, 1 book, and more than 425 international conference presentations, holds 12 patents, and has advised 23 Ph. D. Thesis students (+ 8 on-going), and more than 120 final projects and M.Eng. Theses. According to Publish or Perish (Google Scholar) his publications have received more than 6347/9547 citations, and his h-index is 38 /47 according to Scopus/Google Scholar.

Prof. Adriano Camps is currently the Scientific Coordinator of the CommSensLab "María de Maeztu" Excellence Research Unit, he co-led the Remote Sensing Lab (www.tsc.upc.edu/rs, www.tsc.upc.edu/prsblog) and co-leads the UPC NanoSat Lab (http://www.tsc.upc.edu/nanosatlab). He is the PI of the first four UPC nano-satellites: 1) 3Cat-1, a 1U CubeSat with 7 small technology demonstrators and scientific payloads, 2) 3Cat-2, a 6U CubeSat with the first dual-frequency dual-polarization GNSS-R payload, launched on August 15th 2016 using a Chinese LM-D2 rocket, 3) 3Cat-4, a 1U Cubesat with a software defined radio to implement a microwave radiometer, a GNSS-Reflectomer, and an AIS receiver, and 4) FSSCAT, a tandem mission formed by two 6U CubeSats, overall winner of the Copernicus masters competition 2017.